NANO LETTERS

2004
Vol. 4, No. 8
1535−1539

Size Dependent $\chi^{(3)}$ for Conduction Electrons in Ag Nanoparticles

Vladimir P. Drachev,*,† Andrei K. Buin,‡ Heinz Nakotte,‡ and Vladimir M. Shalaev†

School of Electrical and Computer Engineering, Purdue University, West Lafayette, Indiana 47907, and Physics Department, New Mexico State University, Las Cruces, New Mexico 88003

Received April 15, 2004; Revised Manuscript Received June 30, 2004

ABSTRACT

Our theoretical study of the third-order susceptibility ($\chi^{(3)}$) for Ag dielectric composite reveals a critical role of saturation of optical transitions between discrete states of conduction electrons in metal quantum dots. The calculated size dependence of the $\chi^{(3)}$ for Ag nanoparticles reproduces the published experimental results. Saturation effects lead to a decrease of the local field enhancement factor that is of particular importance for surface-enhanced phenomena, such as Raman scattering and nonlinear optical responses.

Plasmonic nanomaterials have attracted much recent research interest because of their unique optical properties, such as nonlinear optical activity,[1] the chirality of plasmon modes,[2] and the quantum-size effect in two-photon excited luminescence.[3] Current state-of-the-art nanofabrication techniques allow the development of novel applications based on such properties. Of particular importance for applications are the large local-field enhancements for metal particle aggregates that lead to surface-enhanced Raman scattering (SERS) and a number of nonlinear optical phenomena,[4] including the polarization nonlinearities.[5]

The optical response of a nanosized metal particle is a core of all aforementioned phenomena. The confinement of electrons in a metal quantum dot leads to energy quantization of conduction band and appearance of collective plasmon modes. It is well-known that the energy quantization affects most of the physical properties of metal nanoparticles,[6−8] and in particular its nonlinear optical response.[9,10]

The optical properties of a nanosized metal particle can be described in terms of electron transitions between the discrete energy states in a quantum well subjected to the enhanced local field. Large enhancements of the local field inside a particle can be realized at the plasmon resonance frequency. The local field inside a spherical particle, E_i, is related to the applied field, E_0, by the local field (enhancement) factor $f(\omega)$ as follows:[11]

$$E_i = \frac{3\epsilon_h}{\epsilon_m + 2\epsilon_h} E_0 = f(\omega) E_0 \qquad (1)$$

where $\epsilon_m = \epsilon'_m + i\epsilon''_m$ is the complex dielectric response of the metal, and ϵ_h is the dielectric function of a host medium. Note that the zero in the denominator in eq 1 is the surface plasmon resonance condition for a spherical particle embedded in a host.

In a composite with a small volume fraction of metal particles, the third-order nonlinear susceptibility can be computed by[9]

$$\chi^{(3)} = p f(\omega)^2 \, |f(\omega)|^2 \, \chi_m^{(3)} \qquad (2)$$

where p is a volume fraction of the metal particles and $\chi_m^{(3)}$ is the nonlinear susceptibility term of the metal particle itself. It should be noted that both intraband (within conduction band) and interband (between d- and s−p conduction bands) transitions contribute to $\chi_m^{(3)}$. Utilizing the degenerate four-wave mixing technique, the $\chi^{(3)}$ values and its size dependence were extracted from recent detailed experimental studies for nanosized Ag, Au, and Cu particles.[9,12,13] Some of these results were taken to compare the findings with existing theoretical models in order to resolve the origin of the optical nonlinearity. Doing so, it was concluded that the conduction electron intraband transitions play a relatively minor role. This conclusion was based on a theoretical size dependence derived by Hache, Ricard, and Flytzanis (HRF),[9] with the Hamiltonian that uses a description in terms of a vector potential and electron momentum.

In this letter, we will demonstrate that the opposite conclusion can be made if one adopts the quantum well theory with the Hamiltonian of electron-field interaction taking the form

$$H = -\boldsymbol{dE} \qquad (3)$$

where $\boldsymbol{d}$ is the dipole moment and $\boldsymbol{E}$ is the electrical field.

* Corresponding author. Phone: 1-765-494-0628; Fax: 1-765-494-6951. e-mail: vdrachev@ecn.purdue.edu.
† Purdue University.
‡ New Mexico State University.

10.1021/nl049438d CCC: $27.50
Published on Web 07/24/2004

Recently, Rautian[10] showed that, for nanosized spherical particles, the use of the Hamitonian given in eq 3 is preferred, and that this Hamiltonian is no longer equivalent to the standard Hamiltonian in terms of a vector potential. Here, we compare the approaches based on the Rautian and HRF models and calculate the size dependencies of both $\chi_m^{(3)}$ and $f(\omega)$ for nanosized Ag particles. Our results reaffirm the Rautian model, and we find good agreement of the size-dependent $\chi_m^{(3)}$ with the experiment, a result that is not achieved with HRF's approach.

The characteristic separation between the levels near the Fermi energy, E_F, can be estimated as $\delta_F = 2\sqrt{E_F E_0}$, where $E_0 = \hbar^2/2ma^2$ is the energy separation found at the bottom of the conduction band of particles with radius a. Under the condition $\hbar\omega \gg \delta_F$, which is the case for the particle radii ranging from about 2 to about 100 nm and visible frequencies ω, one can distinguish two kinds of transitions between discrete states, resonant ($\omega_{ij} \sim \omega$) and nonresonant ($\omega_{ij} \ll \omega$). The potential saturation of optical transitions between the discrete levels in metal nanoparticle is a second crucial factor. Saturation effects result in a decrease of the local field enhancement factor, and a subsequent decrease in the enhancements for SERS as well as for nonlinear effects.

Using the degenerate electron gas model in an infinite spherical well in the limit $(v_F/2\pi c)\,\lambda \ll a \ll \lambda$ (where v_F is the electron speed near the Fermi surface), Rautian was able to derive the linear and nonlinear dipole moments for a spherical particle induced by field component E_i:

$$d_i = -\frac{e^2 N}{m\omega^2}\left\{F_1\left(1 - i\frac{2\Gamma_2}{\omega}\right) - ig_1\frac{\delta_F}{\hbar\omega} - A_i\left(\frac{ea}{\hbar\omega}\right)^2 I_0\frac{\Gamma_2}{\Gamma_1}\left[F_3\left(1 - i\frac{2\Gamma_2}{\omega}\right) - ig_3\left(\frac{\omega^2}{2\Gamma_2}\right)^2\left(\frac{\delta_F}{\hbar\omega}\right)^5\right]\right\}E_i \quad (4)$$

In eq 4, a denotes the particle radius, ω is the frequency of the field, m is the electron mass, e is the electron charge, N is the number of electrons in the particle, $I_0 = \sum|E_i|^2$, Γ_1 and Γ_2 represent the relaxation rates for the population and coherence, respectively. We focus on a linearly polarized field, where $A_i = 2/5$. For our case, the parameters F_1, g_1, F_3, and g_3 are only weakly size dependent (if at all): F_1 is approximately unity, $g_1 = 0.6$ at $\hbar\omega/E_F \approx 0.5$, F_3 ranges from 0.30 to 0.33 for particles varying between 2 and 15 nm, and $g_3 = 0.64$. A detailed discussion of how to calculate these parameters can be found in ref 10. Basically, the parameters g_1 and g_3 result from the integration over the resonant states, whereas F_1 and F_3 result from the summation of the nonresonant terms close to E_F.[10]

A component *xxxx* of the nonlinear tensor susceptibility, $\chi_{m,xxxx}^{(3)}$ can then be written as the sum of the nonresonant, $\chi_{mn}^{(3)}$, and resonant, $\chi_{mr}^{(3)}$, contributions, i.e.

$$\chi_{m,xxxx}^{(3)}(\omega, -\omega, \omega) = \chi_{mn}^{(3)} + \chi_{mr}^{(3)} \quad (5)$$

Nonresonant contributions can be calculated by integrating over transitions close to the Fermi energy, and resonant contributions are derived by integration from zero to infinity when the energy difference is close to the photon energy. An analysis of eq 4 shows that for linear polarization the two terms in eq 5 are given by

$$\chi_{mn}^{(3)} = \frac{2}{15}\left(\frac{e^2 n}{m\omega^2}\right)\left(\frac{ea}{\hbar\omega}\right)^2\frac{\Gamma_2}{\Gamma_1}\left[1 - i\frac{2\Gamma_2}{\omega}\right]F_3$$

and

$$\chi_{mr}^{(3)} = -i\frac{2}{15}\left(\frac{e^2 n}{m\omega^2}\right)\left(\frac{ea}{\hbar\omega}\right)^2\frac{\Gamma_2}{\Gamma_1}\left(\frac{\omega}{2\Gamma_2}\right)^2\left(\frac{\delta_F}{\hbar\omega}\right)^5 g_3 \quad (6)$$

where n is the electron density. Although $\chi_{mn}^{(3)}$ and $\chi_{mr}^{(3)}$ have different dependencies on the particle size, i.e., $\chi_{mn}^{(3)} \propto a^2$ and $\chi_{mr}^{(3)} \propto a^{-3}$ (note the dependence on a for δ_F), their contributions can be quite similar when dealing with nanosized particles. Underestimating the contribution due to nonresonant transitions can cause an incorrect value and size-dependence for $\chi_m^{(3)}$. To find the magnitudes of $\chi_{mn}^{(3)}$ and $\chi_{mr}^{(3)}$, we need to know the parameters Γ_1 and Γ_2. The electron relaxation in a metal nanoparticle can be expected to be energy- and size-dependent,[14] and it is reasonable to consider the effective relaxation constants as two fitting parameters. Nevertheless, it is useful to obtain some idea about possible ranges of Γ_1 and Γ_2 beforehand. Γ_1 can be extracted from the kinetic rate of the linear optical response or multiphoton electron photoemission under femtosecond excitation. These studies provide a range of values for Γ_1 between 2.5 and 10 cm^{-1} for Ag.[15−17] Γ_2 is sometimes being associated with the mean free path in a metal, which can be deduced from electrical conductivity studies. For bulk Ag, it is found that Γ_2 is of the order of 70 cm^{-1}.[8] It is therefore reasonable to assume that Γ_2 is of the same order of magnitude for nanosized Ag particles.

Figure 1 shows a typical size-dependence for various relaxation constants Γ_2 and for a fixed ratio of $\Gamma_2/\Gamma_1 = 10$.

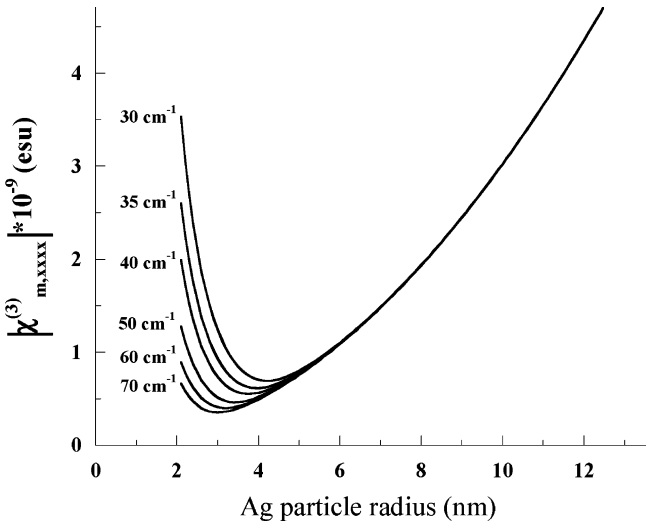

Figure 1. Dependence of $\chi_{m,xxxx}^{(3)}$ on Ag particle size at a fixed ratio of $\Gamma_2/\Gamma_1 = 10$ for various values of Γ_2 ranging from 30 to 70 cm^{-1}.

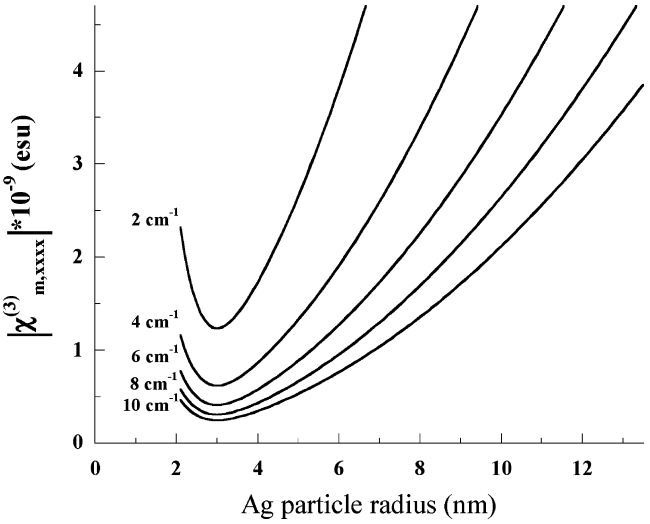

Figure 2. Dependence of $\chi^{(3)}_{m,xxxx}$ on Ag particle size at a fixed value of $\Gamma_2 = 70$ cm^{-1} and various values of Γ_1 ranging from 2 to 10 cm^{-1}.

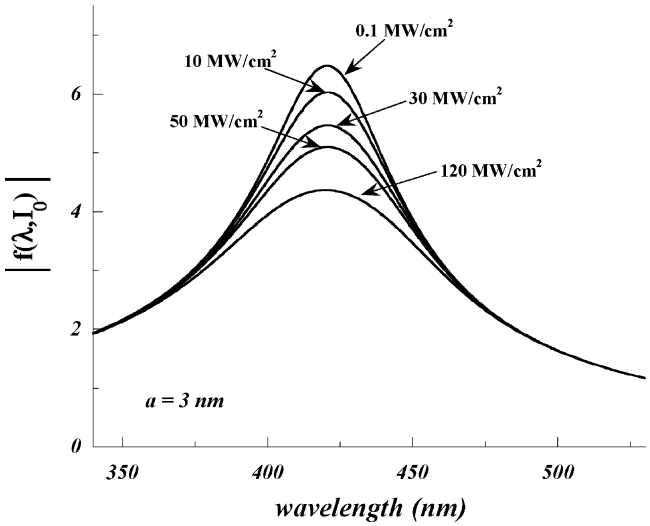

Figure 3. Wavelength dependence of the enhancement factor $f(\lambda,I_0)$ for 3-nm Ag particles at various intensities I_0 ranging from 0.1 to 120 MW/cm^2.

It is obvious from the figure that nonresonant and resonant contributions compete with each other, and this results in the formation of a minimum in $\chi^{(3)}_{m,xxxx}$.

Next, we explored the dependence of $\chi^{(3)}_{m,xxxx}$ for fixed values of Γ_2 at various ratios of Γ_2/Γ_1. An exemplary result is shown in Figure 2, which demonstrates that the position of the minimum is rather insensitive to the ratio Γ_2/Γ_1 and that it is mostly determined by the value Γ_2 in the region of interest.

The calculated size dependence of $\chi^{(3)}_{m,xxxx}$ differs substantially from the behavior predicted by the HRF approach. As will be shown below, their model predicts a continuous decrease of $\chi^{(3)}_{m,xxxx}$ with increasing particle size, with behavior similar to our approach only for very small particle sizes (less than 3 nm or so).

After deriving the expression for $\chi^{(3)}_{m,xxxx}$, the next task remaining is to compute the local field enhancement factor $f(\omega)$, which would allow us then to obtain a value for the third-order nonlinear susceptibility as given in eq 2.

As can be seen from eq 1, the local field enhancement factor can be written as

$$f(\omega) = \frac{3\epsilon_h}{\epsilon_m + 2\epsilon_h} \tag{7}$$

where

$$\epsilon_m = \epsilon_m^0 + 12\,\pi\,\chi_m^{(3)}|f(\omega)|^2 I_0$$

with

$$\epsilon_m^0 = \epsilon_d + 4\pi\,\chi^{(1)}{}_m = \epsilon_d - \left(\frac{4\pi e^2 n}{m\omega^2}\right)\left\{F_1\left[1 - i\frac{2\Gamma_2}{\omega}\right] - ig_1\frac{\delta_F}{\hbar\omega}\right\} \tag{8}$$

Here, ϵ_d is the interband contribution. The zero in the superscripts indicates the linear approximation. Since the medium modifies its properties due to the Kerr effect, higher-order corrections to metal dielectric constants are needed.

As can be seen from eqs 7 and 8, ϵ_m and $f(\omega)$ are coupled, and the local field enhancement factor becomes strongly intensity dependent at high intensities. In general, eq 7 will be cubic on the enhancement factor, and can be solved numerically. After some algebra, eq 7 reads as

$$A|f(\omega)|^6 + B|f(\omega)|^4 + C|f(\omega)|^2 + D = 0 \tag{9}$$

with the coefficients

$$A = c^2 + d^2,\ B = 2(ac + bd),\ C = a^2 + b^2,\ D = -9\epsilon_h^2 \tag{10}$$

The parameters in eq 10 are given as

$$a = \mathrm{Re}(\epsilon_m^0) + 2\epsilon_h,\ b = \mathrm{Im}(\epsilon_m^0),\ c = I_0\,12\pi\mathrm{Re}(\chi_m^{(3)}),\ d = I_0\,12\pi\mathrm{Im}(\chi_m^{(3)}) \tag{11}$$

with $\chi_m^{(3)}$ given by eqs 5 and 6. For given Γ_1 and Γ_2, the solutions at different incident intensities can be computed numerically for different particle sizes and some exemplary results are given in Figures 3 and 4. According to ref 19, $\epsilon_d = 5$, and according to ref 13, $\epsilon_h = 2.2$.

For all particle sizes, there is a decrease in the maximal enhancement factor, even at relatively small intensities. However, the behavior for large particles can be quite different from the one for small particles. For small particles (Figure 3), the position of the maximum in $f(\omega)$ is unchanged, and there is only a decrease of enhancement factor with increasing intensity. For relatively large particles (Figure 4), on the other hand, the resonance condition can be substantially altered as a function of the intensity. This leads to an irregular "distorted" shape for $f(\omega)$, and as a result, nonunique

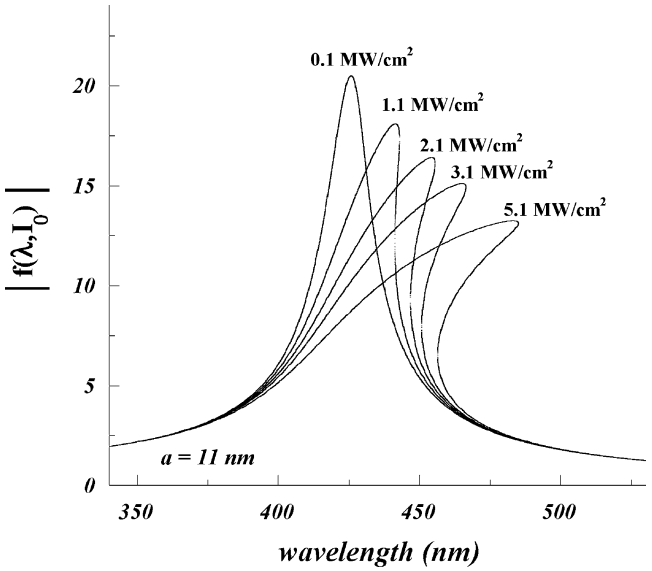

Figure 4. Wavelength dependence of the enhancement factor $f(\lambda,I_0)$ for 11-nm Ag particles at various intensities I_0 ranging from 0.1 to 5.1 MW/cm^2.

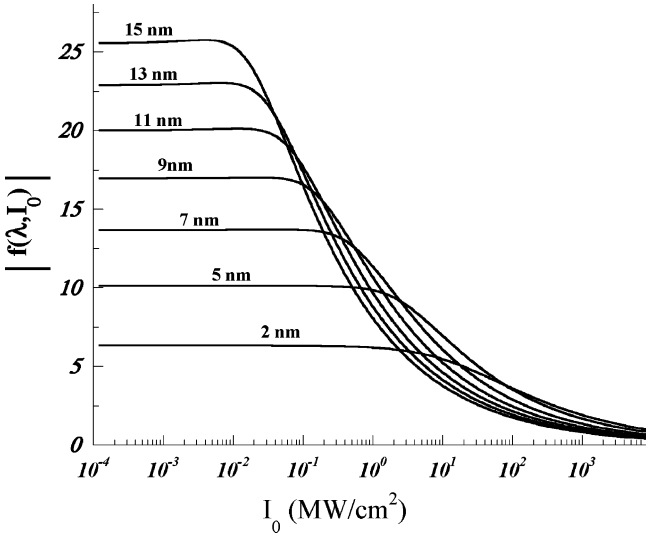

Figure 5. Intensity dependence of the enhancement factor $f(\lambda, I_0)$ for different particle radii ranging from 2 to 15 nm at $\lambda = 420$ nm. Note that a logarithmic *x*-axis is used for clarity.

solutions for the enhancement factor at higher wavelength are possible.

To better understand this behavior, we determine the intensity dependence of the enhancement factor at the surface plasmon wavelength for different particle sizes. The result is shown in Figure 5, and we see that larger particles exhibit saturation effects at far lower intensities when compared to smaller particles. In fact, we find that the saturation manifests itself for the enhancement factor at 100 kW/cm^2 for isolated particles with sizes larger than 7 nm. It is this saturation tendency that is at the origin of the optical bistability (multiple solutions) in materials, as has been discussed by Yoon et al.[18] It should be noted that the formula (8) is generally valid only if nonlinear contributions are small compared with linear ones. At very high intensity, nonlinear contributions higher than third-order have to be taken into account.

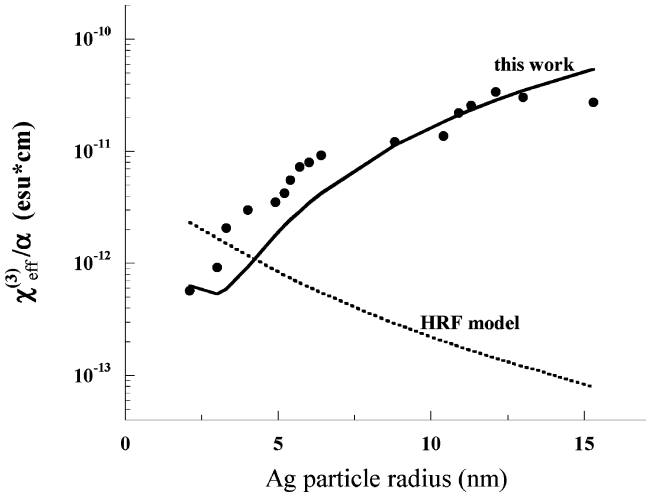

Figure 6. Comparison of the dependence of $\chi^{(3)}_{\text{eff}}/\alpha$ on Ag particle size using two different theoretical approaches, the one discussed in this paper (solid line), and the one based on the HRF model[9] (dashed line), with the experimentally determined values (solid circles) from Uchida et al.[13] Note that a logarithmic *y*-axis has been used for clarity.

Using the computed wavelength dependencies of the enhancement factors as a function of intensity and particle size, we can calculate $\chi^{(3)}_{\text{eff}}/\alpha$, where α is the absorption coefficient and $\chi^{(3)}_{\text{eff}}$ is the experimentally measured nonlinear effective susceptibility of a composite as given in eq 2. The absorption coefficient is related to the volume fraction p since $\alpha = p\omega|f(\omega)|^2\epsilon_m''/nc$, with $n = (\epsilon_h)^{1/2}$. The calculated values of $\chi^{(3)}_{\text{eff}}/\alpha$ are then compared with the experimental results by Uchida et al.[13] The only fitting parameters used in our calculation were Γ_1 and Γ_2, and the intensity I_0 was fixed to the experimental value of 0.1 Mw/cm^2.

Figure 6 shows the experimental data together with our best fit that resulted in reasonable values for $\Gamma_2 \approx 60 \pm 3$ cm^{-1} and $\Gamma_1 \approx 5 \pm 0.2$ cm^{-1}. For comparison, we have also included the predictions arising from the HRF model. Unlike our results, the HRF model predicts a continuous decrease of $\chi^{(3)}_{\text{eff}}/\alpha$ as a function of Ag particle size, which is not corroborated by the experimental data by Uchida et al. Their experimental results were reported without an estimate of potential error bars, and considering the complexity of such experiments relatively large errors (up to 30−50%) could be expected. Even so, we find that the HRF model does not reproduce the experimental results in qualitative size dependence and shows 2 orders of magnitude discrepancy in absolute value for large particles, while our approach is in good agreement with the overall behavior.

Our approach provides additional evidence that the field-induced processes in the conduction band are responsible for the nonlinear behavior of the optical response in Ag nanoparticles. The underlying mechanism is a decrease in the population difference for the coupled energy levels, which ultimately causes the saturation effect for optical transitions in a system with discrete levels. In general, discrete energy levels can be considered if their spectral width, $2\Gamma_2$, is less than the transition energy. For nanosized Ag particles, our best fit yields values for Γ_2 that are more than one order of

magnitude smaller than typical transition energies in the vicinity to E_F.

The decrease in the local-field enhancement factor is a direct consequence of the saturation effects in metal quantum dots. The local field effect introduced phenomenologically through eq 1 implies a linear increase with the field in the particle's dipole moment associated with single electron excitations. The dipole moments cannot grow infinitely with the field; they are limited by the saturation of optical transitions, which causes the decrease of the local field enhancement factor. Formally, this follows from eqs 7 and 8, where the enhancement factor is given as a function of the intensity-dependent susceptibility of metal particles.

In summary, the above model is in good agreement with the observed size dependence of the cubic nonlinearity in the susceptibility for Ag particles. Specifically, we were able to reproduce the experimentally observed size dependence on $\chi_{eff}^{(3)}/\alpha$ using the theoretical treatment proposed by Rautian. This behavior cannot be explained by the HRF approach, which was previously used for the description of experimental results in metal−particle composite systems. Furthermore, our studies emphasize the importance of saturation effects for the local field enhancement factor, which strongly affects nonlinear processes and SERS. The results presented here suggest the saturation of optical transitions in metal nanostructure as the probable reason for a decrease in SERS enhancement. Therefore, the saturation will be especially important when using high-intensity laser light typical for pulsed fs and ps lasers. Finally, we note that the present consideration, emphasizing the role of quantum effects in metal nanoparticles, indicates that revisions for interpretations of several previous experimental observations on optical properties of metal nanoparticles might be needed.

Acknowledgment. This work was supported in part by NSF grants ECS-0210445, DMR-0121814 and by NASA grant NCC-1-01049.

References

(1) Drachev, V. P.; Perminov, S. V.; Rautian, S. G.; Safonov, V. P. *JETP Lett.* **1998**, *68*, 651.
(2) Drachev, V. P.; Bragg, W. D.; Podolskiy, V. A.; Safonov, V. P.; Kim, W.; Ying, Z. C.; Armstrong, R. L.; Shalaev, V. M. *J. Opt. Soc. Am. B* **2001**, *18*, 1896.
(3) Drachev, V. P.; Khaliullin, E. N.; Kim, W.; Alzoubi, F.; Rautian, S. G.; Safonov, V. P.; Armstrong, R. L.; Shalaev, V. M. *Phys. Rev. B* **2004**, *69*, 035318.
(4) Shalaev, V. M. *Nonlinear Optics of Random Media: Fractal Composites and Metal-Dielectric Films*; Springer-Verlag: Heidelberg, 2000.
(5) Drachev, V. P.; Perminov, S. V.; Rautian, S. G.; Safonov, V. P. In *Optical properties of Nanostructured Random Media*; Shalaev, V. M., Ed.; Springer-Verlag: Berlin, 2001; Vol. 82, p 113.
(6) Kawabata, A.; Kubo, R. *J. Phys. Soc. Jpn.* **1966**, *21* 1765.
(7) Gor'kov, L. P.; Eliashberg, G. M. *Sov. Phys. JETP* **1965**, *21*, 940.
(8) Kreibig U.; Volmer, M. *Optical Properties of Metal Clusters*; Springer-Verlag: Berlin, 1995.
(9) Hache, F.; Ricard, D.; Flytzanis, C. *J. Opt. Soc. Am. B* **1986**, *3*, 1647.
(10) Rautian, S. G. *Sov. Phys. JETP* **1997**, *85*, 451.
(11) Jackson, J. D. *Classical Electrodynamics*, 3rd ed.; John Wiley & Sons: New York, 1999.
(12) Bloemer, M. J.; Haus, J. W.; Ashley, P. R. *J. Opt. Soc. Am. B* **1990**, *7*, 790.
(13) Uchida, K.; Kaneko, S.; Omi, S.; Hata, C.; Tanji, H.; Asahara, Y.; Ikushima, A. J. *J. Opt. Soc. Am. B* **1994**, *11*, 1236.
(14) Shahbazyan, T. V.; Perakis, I. E.; Bigot, J. Y. *Phys. Rev. Lett.* **1998**, *81*, 3120.
(15) Groeneveld, R. N. M.; Spirk, R.; Lagendijk, A. *Phys. Rev. B* **1995**, *51*, 11433.
(16) Del Fatti, N.; Bouffanais, R.; Vallee, F.; Flytzanis, C. *Phys. Rev. Lett.* **1998**, *81*, 922.
(17) Lehmann, J.; Merschdorf, M.; Pfeiffer, W.; Thon, A.; Voll, S.; Gerber, G. *J. Chem. Phys.* **2000**, *112*, 5428.
(18) Yoon, Y.-K.; Bennink, R. S.; Boyd, R. W.; Sipe, J. E. *Opt. Comm.* **2000**, *179*, 577.
(19) *Handbook of Optical Constants of Solids*; Palick, E. D., Ed.; Academic Press: New York, 1985.

NL049438D